HHS Public Access

Author manuscript

Int J Radiat Oncol Biol Phys. Author manuscript; available in PMC 2019 September 01.

Published in final edited form as:

Int J Radiat Oncol Biol Phys. 2018 September 01; 102(1): 174–183. doi:10.1016/j.ijrobp.2018.05.032.

High single doses of radiation may induce elevated levels of hypoxia in early-stage non-small cell lung cancer tumors

Olivia J. Kelada, PhD[1,2], **Roy H. Decker, MD, PhD**[1], **Sameer K. Nath, MD**[1], **Kimberly L. Johung, MD, PhD**[1], **Ming-Qiang Zheng, PhD**[3], **Yiyun Huang, PhD**[3], **Jean-Dominique Gallezot, PhD**[3], **Chi Liu, PhD**[3], **Richard E. Carson, PhD**[3], **Uwe Oelfke, PhD**[2], and **David J. Carlson, PhD**[1]

[1]Department of Therapeutic Radiology, Yale University School of Medicine, New Haven, CT, USA

[2]Department of Medical Physics in Radiation Oncology, German Cancer Research Center, Heidelberg, Germany

[3]Department of Radiology and Biomedical Imaging, Yale University School of Medicine, New Haven, CT, USA

Abstract

Purpose—Tumor hypoxia correlates with treatment failure in patients undergoing conventional radiotherapy. However, there are no published studies investigating tumor hypoxia in patients undergoing stereotactic body radiation therapy (SBRT). We aim to non-invasively quantify the tumor hypoxic volume (HV) in non-small cell lung cancer (NSCLC) tumors to elucidate the potential role of tumor vascular response and reoxygenation at high single doses.

Methods—Six SBRT-eligible patients with NSCLC tumors >1 cm were prospectively enrolled in an IRB-approved study. Dynamic positron emission tomography (PET) images were acquired at 0-120 min, 150-180 min, and 210-240 min post-injection of ^{18}F-fluoromisonidazole (^{18}F-FMISO). Serial imaging was performed prior to delivery of 18 Gy, at ~48 hours, and at ~96 hours post-SBRT. Tumor HVs were quantified using a tumor-to-blood ratio (TBR) (>1.2) and rate of tracer influx K_i (> 0.0015 mL·min·cm^{-3}).

Conflict of interest statements:

Olivia J. Kelada: None
Roy H. Decker: None
Sameer K. Nath: None
Kimberly L. Johung: None
Ming-Qiang Zheng: None
Yiyun Huang: None
Jean-Dominique Gallezot: None
Chi Liu: None
Richard E. Carson: None
Uwe Oelfke: None
David J. Carlson: None

Results—An elevated and in some cases persistent level of tumor hypoxia was observed in 3/6 patients. Two patients exhibited no baseline detectable tumor hypoxia, and one patient with high baseline hypoxia only completed 1 imaging session. Based on TBR, in the remaining three patients, tumor HVs increased on day 2 after 18 Gy and then showed variable responses on day 4. In the 3/6 patients with detectable hypoxia at baseline, Baseline tumor HVs ranged between 17-24% (mean: 21%) and HVs on days 2 and 4 ranged between 33-45% (mean: 40%) and 18-42% (mean: 28%), respectively.

Conclusions—High single doses of radiation delivered as part of SBRT may induce an elevated and in some cases persistent state of tumor hypoxia in NSCLC tumors. Hypoxia imaging with ^{18}F-FMISO PET should be used in a larger cohort of NSCLC patients to determine if elevated tumor hypoxia is predictive of treatment failure in SBRT.

Introduction

Stereotactic body radiotherapy (SBRT) has become the primary treatment modality for medically-inoperable early stage NSCLC patients [1]. SBRT consists of the delivery of high single doses of radiation (8-30 Gy per fraction) to the tumor volume in five fractions or fewer using a highly conformal dose distribution through improved target visualization and image guidance [2].

The resistance of hypoxic tumor cells to ionizing radiation has been studied for over 60 years [3]. Tumor hypoxia is prevalent in approximately 90% of solid human tumors, including NSCLC [4,5]. Numerous clinical studies have demonstrated the negative impact of hypoxia on patient outcomes for conventional radiation therapy [6,7]. This clinical radioresistance exists despite allowing for reoxygenation of hypoxic tumor cells between conventional fractions (e.g., 2 Gy per fraction)[8]. To completely overcome hypoxic radioresistance, radiation doses would need to be escalated by up to a factor of 3 to produce the same level of cell kill as under aerobic conditions [9]. However, this is typically not clinically achievable due to normal tissue toxicity.

The clinical impact of tumor hypoxia in the SBRT paradigm remains unclear. SBRT fractionation schemes can vary but are typically delivered in 3-5 fractions [10] with different time intervals between fractions, e.g., 50 Gy in 5 fractions (10 Gy per fraction) over 5-13 days, 48 Gy in 4 fractions (12 Gy per fraction) over 4-8 days, or 45-60 Gy in 3 fractions (15-20 Gy per fraction) over 3-14 days [11–16]. Hypoxia may have a larger impact on treatment outcomes due to the loss of reoxygenation that would occur during conventional radiotherapy [17,18]. Tumor control may be reduced for single doses compared to fractionated radiotherapy for the same biologically effective dose as predicted by classical radiobiological models [17]. It may therefore be desirable to determine an optimal treatment schedule for SBRT according to patient-specific information about the hypoxic status of an individual tumor.

Quantitative molecular imaging can be used to characterize the spatial and temporal variations of hypoxia within human tumors [5]. ^{18}F-fluoromisonidazole (^{18}F-FMISO) positron emission tomography (PET) [19] provides reliable hypoxia quantification methods as the tracer selectively binds in hypoxic cells [20–23]. The objective of this work is to

investigate the effect of high single radiation doses on tumor hypoxia in NSCLC patients using ^{18}F-FMISO PET imaging. This is the first clinical study to quantify changes in hypoxia in human tumors in response to SBRT.

Materials and methods

Patient characteristics

Patients with untreated early stage non-small cell lung cancer (NSCLC) were prospectively enrolled in this pilot study. Six patients (n=6) were accrued between January 2013 and May 2015 with a mean age of 70 years, range 65-78 (patient characteristics shown in Table 1). Single doses of 18 Gy and 10 Gy were selected for this study as these patients received clinical SBRT regimens of either 18 Gy x 3 fractions or 10 Gy x 5 fractions as standard of care [10]. All patients gave written consent prior to study participation. The study was approved by the Yale University Human Investigation Committee. All patients were treated with an SBRT regimen according to institutional protocols. Poor patient compliance prevented patient 1 from completing the imaging protocol.

^{18}F-FMISO PET image acquisition and analysis

The PET/CT imaging protocol is shown in Figure 1. PET/CT scans were performed on a four-ring Siemens Biograph mCT scanner (Siemens Medical Solutions, Knoxville, TN, USA). Each patient underwent three single-bed dynamic PET/CT scans of the thorax. Images were acquired from 0-120 min, 150-180 min, and 210-240 min post-injection with a CT performed before each imaging session for attenuation correction. This scanning protocol was performed on days 0, 2 and 4, corresponding to a baseline scan immediately prior to the first fraction of SBRT, 2 days after the first fraction, and 4 days after the first fraction, respectively. A respiratory-gated 4D-CT was acquired on the final day after PET imaging and used to measure the magnitude of respiratory motion.

Patients were imaged supine, head-first, and immobilized in a personalized Vac-lok™ bag to provide reproducible setup between imaging sessions and treatment position. An intravenous line was placed to deliver a bolus injection of ~5 mCi of ^{18}F-FMISO, which was prepared by published methods [24]. An Anzai system (Anzai Medical, Tokyo, Japan) was attached to the lower abdomen to measure the respiratory signal.

List mode data were divided into frames of 6x30 sec; 3x1 min; 2x2 min; and 34x5 min. Each 3D volume of the dynamic PET image series was reconstructed into a 400×400×111 matrix (voxel dimensions, 2.036×2.036×2 mm) using a OP-OSEM algorithm incorporated with point spread function, time-of-flight information, and a 3.0 mm FWHM Gaussian isotropic post-reconstruction filter. Corrections for dead time, random coincidences, and scatter were applied for each frame. A 3D low-dose CT was acquired for attenuation correction. PET scans were co-registered to correct for body motion between same-day scans.

To create respiratory-corrected images, the PET listmode data acquired from 210-240 min was retrospectively binned into 8 phase frames (gates) according to patient Anzai respiratory signals. Maximum motion was defined by observing and measuring movement of one tumor point between inspiration and expiration gates of the 4DCT. The end-expiration gate was

selected by viewing the coronal slice for each respiratory phase gate and selecting the phase where the liver position was the highest.

MEDx 7.1 (Medical Numerics, Sterling, VA) was used to visualize and process dynamic images. Image-derived input functions were identified by drawing a Region of Interest (ROI) on the transaxial slices containing the left ventricle (LV) blood pool in frames acquired < 2 min post-injection. The LV blood pool ROI was then applied to the dynamic PET dataset to generate an input function using the average activity. The heart time-activity curve (TAC), after its peak, was fitted using the sum of exponential functions (1-3 exponentials, automatically determined by minimizing the chi-square criterion) to reduce noise for more accurate kinetic analysis.

Absolute tumor volume was defined on the baseline low-dose pre-PET CT. Tumor diameter was measured on CT and tumor hypoxia ROI was drawn on the summed 210-240 min frame of the dynamic PET data for maximum ^{18}F-FMISO binding.

The tumor hypoxic volume (HV) (using tumor-to-blood ratio, TBR) was calculated on the end-expiration gate summed 210-240 min image. The HV is defined as the ratio of the number of hypoxic voxels based on ^{18}F-FMISO imaging at each time point to the total number of tumor voxels based on pre-treatment CT imaging. Therefore, the denominator of this ratio is constant across all imaging time points. It is important to note that the HV is different from the hypoxic fraction (HF) of a tumor, which is defined as the fraction of viable clonogenic cells in a tumor that are resistant to radiation due to hypoxia. The voxel uptake values (in the tumor hypoxia ROI) were divided by the average input function value from 210-240 min post-injection to create a TBR value for each tumor voxel. Mean and maximum TBR values were calculated over the entire tumor ROI. A TBR threshold of 1.2 was used to assign voxels to the tumor HV [25]. Dynamic data uncorrected for respiratory motion were fit to two-tissue compartment (2TC) [22] and Patlak [26] models to estimate tracer kinetic parameters ($t^* = 40$ min). The rate of tracer perfusion, K_1 (mL·min·cm^{-3}), and the net rate of tracer binding and influx, K_i (mL·min·cm^{-3}), were estimated for each voxel. Mean values were calculated over the entire tumor ROI. Levenberg–Marquardt least-squares optimization algorithm was used to estimate model parameters in each voxel. HVs were also quantified using a K_i threshold of > 0.0015 mL·min·cm^{-3} (selected based on patient baseline images). TBR images and parametric maps were generated in MATLAB.

Results

All patient characteristics are shown in Table 1. The temporal variation in tumor HV for all patients and mean and maximum TBR for all tumors is shown in Table 2. 3/5 patients who completed the imaging protocol had detectable baseline tumor hypoxia (patients 2, 5, and 6). Excluding patient 1 (incomplete imaging protocol) and patients 3 and 4 (no baseline hypoxia, $K_1 > 0$, see discussion), baseline tumor HVs ranged between 17-24% (mean: 21%). HVs on days 2 and 4 ranged between 33-45% (mean: 40%) and between 18-42% (mean: 28%), respectively. Between scans on days 0 and 2, mean HV consistently increased. However, between scans acquired on days 2 and 4, a variable decrease was observed. For patients 2, 5, and 6, tumor HVs increased by up to a factor of 2.7 post-SBRT delivery

(between baseline and day 2 of imaging). On day 4, 96 hours post-SBRT, the tumor HV either decreased to baseline (patient 2 and 6) or was effectively unchanged (patient 5).

Transaxial images for all patients with detectable baseline hypoxia are shown in Figure 2. CT images highlighting the tumor volumes are shown in 2A, 5A, and 6A. Tumor hypoxia PET images, as quantified by TBR estimated from 210-240 min, are shown in 2B, 5B, and 6B without respiratory motion correction and 2C, 5C, and 6C corrected for respiratory motion. In patients 2, 5, and 6, we observed a large increase in HV post-SBRT, i.e., SBRT induced an elevated level of tumor hypoxia for all patients with detectable baseline hypoxia. Enlarged transaxial tumor regions and the corresponding temporal variation in tumor HV are shown in Figure 3.

The results of a tracer kinetic analysis of ^{18}F-FMISO are shown in Figure 4. Axial images of the rate of net tracer influx K_i (mL·min·cm^{-3}) for patients 2, 5 and 6 are shown in the **top panel** in rows A, B, and C, respectively. For patient 2, the observed trend in HV variation calculated using K_i >0.0015 is the same as the trend in HV observed using conventional static imaging metrics (i.e., TBR >1.2). However, a change in the temporal pattern in HV is observed in patients 5 and 6 when using K_i quantification compared to TBR. The temporal variation in HVs calculated using tracer kinetics (K_i > 0.0015) between imaging days for all patients with detectable baseline hypoxia is shown in Figure 4, **bottom panel**. Baseline HVs ranged between 18-23% (mean: 20.3%). HVs on day 2 and day 4 ranged between 20%-48% (mean: 35.8%) and between 26%-69% (mean: 41.2%), respectively. In agreement with trends in the TBR quantification, an increase in mean HVs for all three patients between day 0 (20.3%) and day 2 (35.8%) is also observed using K_i, metrics. However, a comparison of the mean HV between day 2 (35.8%) and day 4 (41.2 %) indicates a further increase in HV while TBR results suggest a decrease in mean HV on day 4.

Discussion

This is the first study to suggest that large single doses of radiation delivered as part of an SBRT treatment course may induce elevated and in some cases persistent levels of hypoxia in human tumors. Our preliminary results imply that NSCLC patients with detectable baseline levels of tumor hypoxia may have an elevated level of tumor hypoxia (by up to a factor of 2.7) two days after receiving the first fraction of SBRT. It has already been shown that tumor hypoxia may result in a larger decrease in biological effectiveness for hypofractionated regimens, such as SBRT, than for conventional fractionation [17,18]. Fractionation reduces hypoxic radioresistance in tumors by allowing for reoxygenation between doses [27]. However, for NSCLC patients treated with SBRT, local tumor control rates can be >90% at 3 years [11], and the impact of tumor hypoxia on clinical outcomes remains unclear and even controversial [28].

The observed increase in HV two days post-delivery of a single SBRT fraction in patients with baseline detectable hypoxia suggests that tumor hypoxia may play a role in the SBRT paradigm. In the absence of reoxygenation, the HV (defined as the ratio of the number of hypoxic voxels based on ^{18}F-FMISO imaging at each time point to the total number of tumor voxels based on pre-treatment CT imaging) would remain the same on day 0 and day

2 assuming the same total tumor volume (defined by CT) across all imaging days. If reoxygenation were occurring between fractions (as might normally be expected in the absence of SBRT-induced hypoxia), then we would expect to observe a reduction in the HV on day 2, not an increase. This further supports the possibility in our view that high SBRT doses can induce an increase in tumor hypoxia despite some level of tumor reoxygenation.

The impact of radiation on functional vascularity, reoxygenation, and vascular changes has been studied extensively in murine tumors [29–32]. Preclinical data [28,33,34] supports the observation that HV increases two days post-SBRT delivery and tumor reoxygenation has been measured experimentally in a number of preclinical animal models after the delivery of a single high dose of radiation. Kallman et al. [27] reported that reoxygenation occurs rapidly in animal tumors, with hypoxic fractions starting at 100% immediately after 15 Gy of irradiation and declining quickly by 1 hour and thereafter. Park et al. [28] concluded that irradiation of tumors with 5 to 10 Gy in a single dose causes mild vascular damage, whereas increasing the radiation dose to higher than 10 Gy per fraction induces severe vascular destruction. Song et al. [33] found that intratumor perfusion of Hoechst 33342 was markedly reduced, and blood vessel morphology was altered at 6 hours after high dose radiation in lung tumors. Yet, two days after radiation (the same time-point used in our study), Hoechst 33342 perfusion and CD31 density were partly restored but still significantly decreased compared to prior to radiation delivery. In addition, Song and Cho et al. [34] found the frequency of blood vessels perfused with Hoechst 33342 dye was significantly reduced 2 days after 20 Gy irradiation, demonstrating that tumor blood vessels were severely occluded. Moreover, many CD31-positive blood vessels in the irradiated tumors were devoid of Hoechst 33342 dye, demonstrating that the endothelial cells were still viable but the blood vessels were static. Levels of CA9, a marker for hypoxic cells significantly increased as early as 1 day after 20-Gy irradiation suggesting that the intratumor microenvironment was hypoxic as a result of the vascular damage. These preclinical studies have demonstrated that tumor vasculature does respond differently at high single doses compared to low doses. This could suggest that SBRT induces a vascular response that results in an increase in tumor hypoxia. However, no previous study has investigated changes in the vascular response and hypoxic status of human tumors in response to high single doses of radiation.

To measure the change in HV after SBRT delivery, two quantification methods were used to calculate the tumor hypoxic volume and imaging data was corrected for respiratory motion. Thorwarth et al. [35] and others [36,37] have suggested irreversible kinetic modeling of ^{18}F-FMISO dynamic PET data may provide more accurate tumor hypoxia quantification by accounting for tracer delivery to the tumor (K_1) and binding to hypoxic cells (k_3 or K_i) [35], which is especially important for non-homogenously perfused tumors [38]. K_1 describes transport from the vascular compartment into the extravascular tissue compartment, and there is some evidence that it is a surrogate biomarker of tumor perfusion of the tracer at the time of imaging [39]. Our results suggest that ^{18}F-FMISO successfully ($K_1 > 0$) perfused into all patient tumors and that out of five patients who completed the imaging protocol, two patients had undetectable baseline levels of hypoxia (HV=0%) despite a comparable rate of tumor perfusion of the tracer ($K_1 > 0$). This lack of detectable hypoxia in patients 3 and 4 is due to a lack of tracer binding and not inadequate tracer availability. This observed heterogeneity in baseline hypoxia is consistent with many previous studies demonstrating

heterogeneous levels of hypoxia in human tumors [4]. Unlike K_i, TBR only provides a composite map of peripheral tracer clearance. TBR does not account for the impact of tracer delivery and clearance in the tumor, nor does it reflect the irreversible tracer binding in the presence of hypoxia [25,40]. This may explain the variation in mean HVs between day 2 and 4 when comparing TBR to kinetic modeling methods. Respiratory motion during PET acquisition could have affected the voxel TACs and K_i parameter quantification. The maximum observed tumor motion was in patients with lower lobe tumors, patients 3 (12.4 mm) and 6 (14.6 mm). All others had upper lobe tumors with reduced tumor motion [41]. Patient 2 exhibited the same trend in variation in HV post-SBRT between respiratory-corrected and uncorrected images and this may be attributed to the maximum magnitude of motion for this patient (4.8 mm) being approximately equal to the intrinsic resolution (4 mm). Respiratory motion correction has been previously shown to impact estimated kinetic parameters for dynamic PET imaging in the thorax [42]. Respiratory-correction of the dynamic data may have impacted patient 6, and this could explain the observed differences between quantification of HV using TBR >1.2 and $K_i > 0.0015$. The impact of respiratory motion on tracer kinetic model parameters must be further investigated in future ^{18}F-FMISO PET modeling studies.

Although we are unable to draw statistical conclusions from this small and heterogeneous dataset, the main observation of this study that high single doses of radiation can induce hypoxia is novel as it still remains unclear whether SBRT treatment has overcome the problem of tumor hypoxia. While SBRT has been shown to provide high rates of local control for early-stage NSCLC patients, the mechanisms of treatment response are still largely debated in the community [18]. Are the high doses of ionizing radiation used in SBRT inducing more DNA damage in aerobic and hypoxic tumor cells, i.e. are technical advances in SBRT treatments allowing the delivery of high biologically effective doses? Or are secondary mechanisms of tumor control, e.g., increased vascular damage or systemic immune responses, contributing to the excellent local control rates above and beyond the classical mechanisms of treatment response? It is critical to study changes in tumor oxygenation in this patient cohort to help guide future clinical studies aimed at answering these questions. A previously study [17] suggested that tumor hypoxia could be more detrimental for hypofractionated regimens, such as SBRT. This could be due to a reduction in time for reoxygenation to occur between fractions [43]. Fractionation schedules currently vary widely in clinical practice. For example, RTOG 0236 (the basis for current clinical practice), suggests an SBRT dose prescription of 54 Gy in 3 fractions of 18 Gy, with all three fractions delivered within 2 weeks [11,44]. While Nagata et al. [12] prescribed 12 Gy per fraction × 4 over 5–13 days and Chang et al. [14] delivered 50 Gy over 4 consecutive days i.e. 12.5 Gy every day for 4 days. A meta-analysis of recent clinical data from patients with brain metastases and heterogeneous hypoxia status suggest that *multi*-fraction SBRT provides better tumor control than single-fraction regimens [16]. Also, a schedule of 5 fractions of 10 Gy delivered every other day (excluding weekends) has been shown also been to increase local control when compared consecutive daily fractions [10,45]. This disparity in fractionation and total treatment time has not been carefully studied. No clinical study to date has measured the effect of SBRT on tumor hypoxia in NSCLC patients to elucidate whether the efficacy of SBRT relies on reoxygenation.

It is widely accepted that PET imaging can be used to quantify tumor hypoxia and stratify patients into responding and non-responding subgroups to provide more targeted treatments for patients with poor prognosis [46]. NSCLC patients undergoing SBRT may, in particular, benefit from stratification according to hypoxic status, as shown by others using ^{18}F-FMISO PET imaging for conventional radiation treatments [47]. However, in clinical practice, the hypoxic status of individual tumors is not considered when designing fractionation schedules. As previously mentioned, patients with more hypoxic tumors could account for local failures in SBRT for NSCLC. The increase in HV observed two days post-SBRT treatment in this study suggests tumor oxygenation should be considered when identifying the optimal SBRT fractionation. To overcome hypoxic radioresistance, the SBRT delivery schedule for patients with more hypoxic tumors could be altered from three times per week to once per week for three weeks. Increasing the time between fractions may allow for more reoxygenation to occur and improve clinical outcomes [45]. Routine quantification of tumor hypoxia in SBRT patients will be necessary to elucidate the impact on patient outcomes. In turn, hypoxia imaging could be used to develop personalized treatments, e.g, de-escalation of prescription doses could reduce the risk of normal tissue complications in patients with low levels of hypoxia. This strategy has been successful in H&N cancer patients who received selectively de-escalated doses to neck nodes based on hypoxia imaging results to achieve 100% locoregional control [48]. The selection of less resistant tumors for dose de-escalation could increase the eligibility of patients with more central lesions for SBRT. Also, hypoxia-selective drugs, e.g., tirapazamine [49], could counteract the radioprotective effect of tumor hypoxia following delivery of the first fraction. Alternatively, hypoxic cell radiosensitizers administered immediately prior to SBRT dose delivery could sensitize patients with hypoxic tumors [17,50]. These drugs were mostly unsuccessful with conventional fractionation schedules [51] but could achieve more cell kill in the SBRT paradigm as sensitizer enhancement ratios are higher for larger radiation doses [17,50] and have been shown to be well tolerated with single or a few large doses [52]. Dose escalation has also been proposed to overcome resistance [53] but this method still faces a number of technical difficulties [5].

Larger studies with more patients must be performed to confirm the suggestive results reported in this study. However, the results presented in this pilot study provide strong motivation for further investigation and clinical implementation of the selection of optimal fractionation regimens for SBRT patients allowing for maximum tumor oxygenation at the time of treatment delivery. In addition, future studies could provide valuable insight into the clinical role of vascular changes in treatment response by correlating clinical outcomes with serial hypoxia imaging in larger patient cohorts.

Conclusion

This is the first study to suggest that large single doses delivered as part of SBRT may induce elevated and in some cases persistent levels of hypoxia in human tumors. Results show heterogeneity in baseline hypoxia and demonstrate an increase in tumor hypoxia post-SBRT delivery for patients with detectable baseline hypoxia. Further research is needed to determine if stratification by tumor hypoxia status may benefit NSCLC patients undergoing

SBRT and if strategies to individualize treatments could further improve tumor control and reduce normal tissue toxicity.

Acknowledgments

This work was supported by a Yale Cancer Center Pilot grant, Yale PET center Pilot funds, and a Helmholtz International Graduate School PhD Fellowship. This work was also supported by NIH grants 1S10RR029245-01 and by CTSA Grant Number UL1 TR000142 from the National Center for Advancing Translational Science, a component of the National Institutes.

References

1. Iyengar P, Westover K, Timmerman RD. Stereotactic ablative radiotherapy (sabr) for non-small cell lung cancer. Seminars in respiratory and critical care medicine. 2013; 34:845–854. [PubMed: 24258574]
2. Lo SS, et al. Stereotactic body radiation therapy: A novel treatment modality. Nat Rev Clin Oncol. 2010; 7:44–54. [PubMed: 19997074]
3. Gray LH, et al. The concentration of oxygen dissolved in tissues at the time of irradiation as a factor in radiotherapy. Br J Radiol. 1953; 26:638–648. [PubMed: 13106296]
4. Brown JM, Wilson WR. Exploiting tumour hypoxia in cancer treatment. Nat Rev Cancer. 2004; 4:437–447. [PubMed: 15170446]
5. Kelada OJ, Carlson DJ. Molecular imaging of tumor hypoxia with positron emission tomography. Radiat Res. 2014; 181:335–349. [PubMed: 24673257]
6. Nordsmark M, Overgaard M, Overgaard J. Pretreatment oxygenation predicts radiation response in advanced squamous cell carcinoma of the head and neck. Radiother Oncol. 1996; 41:31–39. [PubMed: 8961365]
7. Brizel DM, et al. Oxygenation of head and neck cancer: Changes during radiotherapy and impact on treatment outcome. Radiother Oncol. 1999; 53:113–117. [PubMed: 10665787]
8. Kallman RF, Dorie MJ. Tumor oxygenation and reoxygenation during radiation therapy: Their importance in predicting tumor response. Int J Radiat Oncol Biol Phys. 1986; 12:681–685. [PubMed: 3700172]
9. Carlson DJ, Stewart RD, Semenenko VA. Effects of oxygen on intrinsic radiation sensitivity: A test of the relationship between aerobic and hypoxic linear-quadratic (lq) model parameters. Med Phys. 2006; 33:3105–3115. [PubMed: 17022202]
10. Corso CD, et al. Stage i lung sbrt clinical practice patterns. American journal of clinical oncology. 2014
11. Timmerman R, et al. Stereotactic body radiation therapy for inoperable early stage lung cancer. Jama. 2010; 303:1070–1076. [PubMed: 20233825]
12. Nagata Y, et al. Clinical outcomes of a phase i/ii study of 48 gy of stereotactic body radiotherapy in 4 fractions for primary lung cancer using a stereotactic body frame. Int J Radiat Oncol Biol Phys. 2005; 63:1427–1431. [PubMed: 16169670]
13. Fakiris AJ, et al. Stereotactic body radiation therapy for early-stage non-small-cell lung carcinoma: Four-year results of a prospective phase ii study. Int J Radiat Oncol Biol Phys. 2009; 75:677–682. [PubMed: 19251380]
14. Chang JY, et al. Stereotactic body radiation therapy in centrally and superiorly located stage i or isolated recurrent non-small-cell lung cancer. Int J Radiat Oncol Biol Phys. 2008; 72:967–971. [PubMed: 18954709]
15. Chaudhuri AA, et al. Stereotactic ablative radiotherapy (sabr) for treatment of central and ultra-central lung tumors. Lung cancer. 2015; 89:50–56. [PubMed: 25997421]
16. Shuryak I, et al. High-dose and fractionation effects in stereotactic radiation therapy: Analysis of tumor control data from 2965 patients. Radiother Oncol. 2015
17. Carlson DJ, et al. Hypofractionation results in reduced tumor cell kill compared to conventional fractionation for tumors with regions of hypoxia. Int J Radiat Oncol Biol Phys. 2011; 79:1188–1195. [PubMed: 21183291]

18. Brown JM, Carlson DJ, Brenner DJ. The tumor radiobiology of srs and sbrt: Are more than the 5 rs involved? Int J Radiat Oncol Biol Phys. 2014; 88:254–262. [PubMed: 24411596]
19. Rasey JS, et al. Radiolabelled fluoromisonidazole as an imaging agent for tumor hypoxia. Int J Radiat Oncol Biol Phys. 1989; 17:985–991. [PubMed: 2808061]
20. Koh WJ, et al. Imaging of hypoxia in human tumors with [f-18]fluoromisonidazole. Int J Radiat Oncol Biol Phys. 1992; 22:199–212. [PubMed: 1727119]
21. Valk PE, et al. Hypoxia in human gliomas: Demonstration by pet with fluorine-18-fluoromisonidazole. J Nucl Med. 1992; 33:2133–2137. [PubMed: 1334136]
22. Rasey JS, et al. Quantifying regional hypoxia in human tumors with positron emission tomography of [18f]fluoromisonidazole: A pretherapy study of 37 patients. Int J Radiat Oncol Biol Phys. 1996; 36:417–428. [PubMed: 8892467]
23. Rasey JS, et al. Determining hypoxic fraction in a rat glioma by uptake of radiolabeled fluoromisonidazole. Radiat Res. 2000; 153:84–92. [PubMed: 10630981]
24. Zheng MQ, et al. Synthesis of [(18)f]fmiso in a flow-through microfluidic reactor: Development and clinical application. Nucl Med Biol. 2015; 42:578–584. [PubMed: 25779036]
25. Kelada OJ, et al. Quantification of tumor hypoxic fractions using positron emission tomography with [18f]fluoromisonidazole ([18f]fmiso) kinetic analysis and invasive oxygen measurements. Mol Imaging Biol. 2017; 19:893–902. [PubMed: 28409339]
26. Patlak CS, Blasberg RG, Fenstermacher JD. Graphical evaluation of blood-to-brain transfer constants from multiple-time uptake data. J Cereb Blood Flow Metab. 1983; 3:1–7. [PubMed: 6822610]
27. Kallman RF. The phenomenon of reoxygenation and its implications for fractionated radiotherapy. Radiology. 1972; 105:135–142. [PubMed: 4506641]
28. Park HJ, et al. Radiation-induced vascular damage in tumors: Implications of vascular damage in ablative hypofractionated radiotherapy (sbrt and srs). Radiat Res. 2012; 177:311–327. [PubMed: 22229487]
29. Clement JJ, Song CW, Levitt SH. Changes in functional vascularity and cell number following x-irradiation of a murine carcinoma. Int J Radiat Oncol Biol Phys. 1976; 1:671–678. [PubMed: 977401]
30. Clement JJ, Tanaka N, Song CW. Tumor reoxygenation and postirradiation vascular changes. Radiology. 1978; 127:799–803. [PubMed: 663181]
31. Song CW, Levitt SH. Effect of x irradiation on vascularity of normal tissues and experimental tumor. Radiology. 1970; 94:445–447. [PubMed: 5412822]
32. Song CW, et al. Vascular changes in neuroblastoma of mice following x-irradiation. Cancer Res. 1974; 34:2344–2350. [PubMed: 4843534]
33. Song C, et al. Real-time tumor oxygenation changes after single high-dose radiation therapy in orthotopic and subcutaneous lung cancer in mice: Clinical implication for stereotactic ablative radiation therapy schedule optimization. Int J Radiat Oncol Biol Phys. 2016; 95:1022–1031. [PubMed: 27130790]
34. Song CW, et al. Indirect tumor cell death after high-dose hypofractionated irradiation: Implications for stereotactic body radiation therapy and stereotactic radiation surgery. Int J Radiat Oncol Biol Phys. 2015; 93:166–172. [PubMed: 26279032]
35. Thorwarth D, et al. A kinetic model for dynamic [18f]-fmiso pet data to analyse tumour hypoxia. Phys Med Biol. 2005; 50:2209–2224. [PubMed: 15876662]
36. Kelly CJ, Brady M. A model to simulate tumour oxygenation and dynamic [18f]-fmiso pet data. Phys Med Biol. 2006; 51:5859–5873. [PubMed: 17068369]
37. Wang W, et al. Evaluation of a compartmental model for estimating tumor hypoxia via fmiso dynamic pet imaging. Phys Med Biol. 2009; 54:3083–3099. [PubMed: 19420418]
38. Taylor E, et al. Quantifying hypoxia in human cancers using static pet imaging. Phys Med Biol. 2016; 61:7957–7974. [PubMed: 27779123]
39. Bartlett RM, et al. Image-guided po2 probe measurements correlated with parametric images derived from 18f-fluoromisonidazole small-animal pet data in rats. J Nucl Med. 2012; 53:1608–1615. [PubMed: 22933821]

40. McGowan DR, et al. 18 f-fluoromisonidazole uptake in advanced stage non-small cell lung cancer: A voxel-by-voxel pet kinetics study. Med Phys. 2017; 44:4665–4676. [PubMed: 28644546]
41. Seppenwoolde Y, et al. Precise and real-time measurement of 3d tumor motion in lung due to breathing and heartbeat, measured during radiotherapy. Int J Radiat Oncol Biol Phys. 2002; 53:822–834. [PubMed: 12095547]
42. Yu Y, et al. Event-by-event continuous respiratory motion correction for dynamic pet imaging. J Nucl Med. 2016; 57:1084–1090. [PubMed: 26912437]
43. Fowler JF, et al. Optimum fractionation of the c3h mouse mammary carcinoma using x-rays, the hypoxic-cell radiosensitizer ro-07-0582, or fast neutrons. Int J Radiat Oncol Biol Phys. 1976; 1:579–592. [PubMed: 977399]
44. Radiation therapy oncology group 0236. A phase ii trial of stereotactic body radiation therapy (sbrt) in the treatment of patients with medically inoperable stage i/ii non-small cell lung cancer. RTOG Foundation; Https://www.Rtog.Org/clinicaltrials/protocoltable/studydetails.Aspx?Study=0236:
45. Alite F, et al. Local control dependence on consecutive vs. Nonconsecutive fractionation in lung stereotactic body radiation therapy. Radiother Oncol. 2016; 121:9–14. [PubMed: 27543255]
46. Overgaard J. Hypoxic modification of radiotherapy in squamous cell carcinoma of the head and neck–a systematic review and meta-analysis. Radiother Oncol. 2011; 100:22–32. [PubMed: 21511351]
47. Sachpekidis C, et al. Combined use of (18)f-fdg and (18)f-fmiso in unresectable non-small cell lung cancer patients planned for radiotherapy: A dynamic pet/ct study. Am J Nucl Med Mol Imaging. 2015; 5:127–142. [PubMed: 25973334]
48. Lee N, et al. Strategy of using intratreatment hypoxia imaging to selectively and safely guide radiation dose de-escalation concurrent with chemotherapy for locoregionally advanced human papillomavirus-related oropharyngeal carcinoma. Int J Radiat Oncol Biol Phys. 2016; 96:9–17. [PubMed: 27511842]
49. Rischin D, et al. Prognostic significance of [18f]-misonidazole positron emission tomography-detected tumor hypoxia in patients with advanced head and neck cancer randomly assigned to chemoradiation with or without tirapazamine: A substudy of trans-tasman radiation oncology group study 98.02. J Clin Oncol. 2006; 24:2098–2104. [PubMed: 16648512]
50. Brown JM, Diehn M, Loo BW Jr. Stereotactic ablative radiotherapy should be combined with a hypoxic cell radiosensitizer. Int J Radiat Oncol Biol Phys. 2010; 78:323–327. [PubMed: 20832663]
51. Tepper JE, et al. The role of misonidazole combined with intraoperative radiation therapy in the treatment of pancreatic carcinoma. J Clin Oncol. 1987; 5:579–584. [PubMed: 3559650]
52. Drzymala RE, et al. A phase i-b trial of the radiosensitizer: Etanidazole (sr-2508) with radiosurgery for the treatment of recurrent previously irradiated primary brain tumors or brain metastases (rtog study 95-02). Radiother Oncol. 2008; 87:89–92. [PubMed: 18342381]
53. Lin Z, et al. The influence of changes in tumor hypoxia on dose-painting treatment plans based on 18f-fmiso positron emission tomography. Int J Radiat Oncol Biol Phys. 2008; 70:1219–1228. [PubMed: 18313529]

Summary

Tumor hypoxia is non-invasively quantified in early-stage non-small cell lung cancer patients undergoing stereotactic body radiotherapy (SBRT) to elucidate the role of tumor vascular response and reoxygenation at high single doses. We observe heterogeneity in baseline hypoxia and an increase in tumor hypoxia post-SBRT for patients with detectable baseline hypoxia. High single doses of radiation delivered as part of SBRT may induce an elevated and in some cases persistent state of tumor hypoxia in NSCLC tumors.

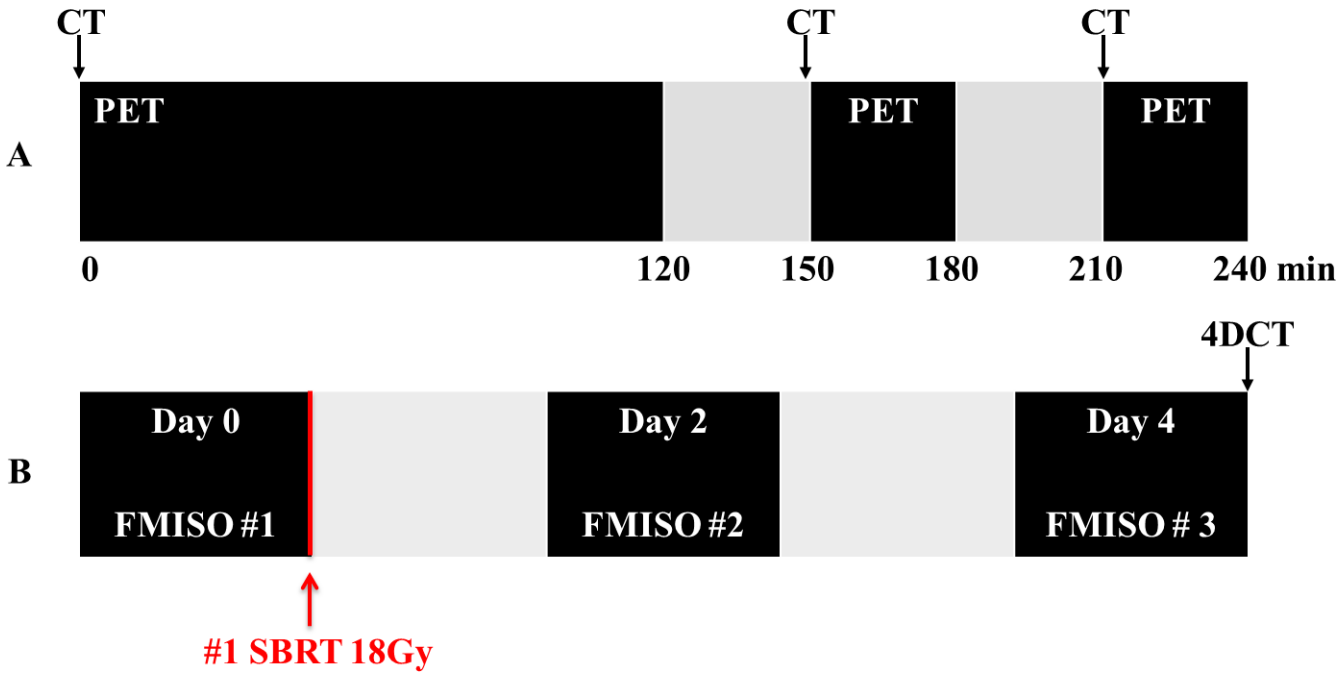

Figure 1.

PET/CT imaging protocol. **A**: Three dynamic ^{18}F-FMISO PET scans were preformed from 0-120 min, 150-180 min, and 210-240 min post-injection, each preceded by a low-dose CT for attenuation correction. **B**: Serial imaging was performed around a single SBRT fraction. PET/CT was acquired immediately prior to the first fraction (day 0). Subsequent scans on days 2 and 4 were acquired ~48 hours and ~96 hours after the first fraction of SBRT, respectively. A 4DCT was acquired on day 4.

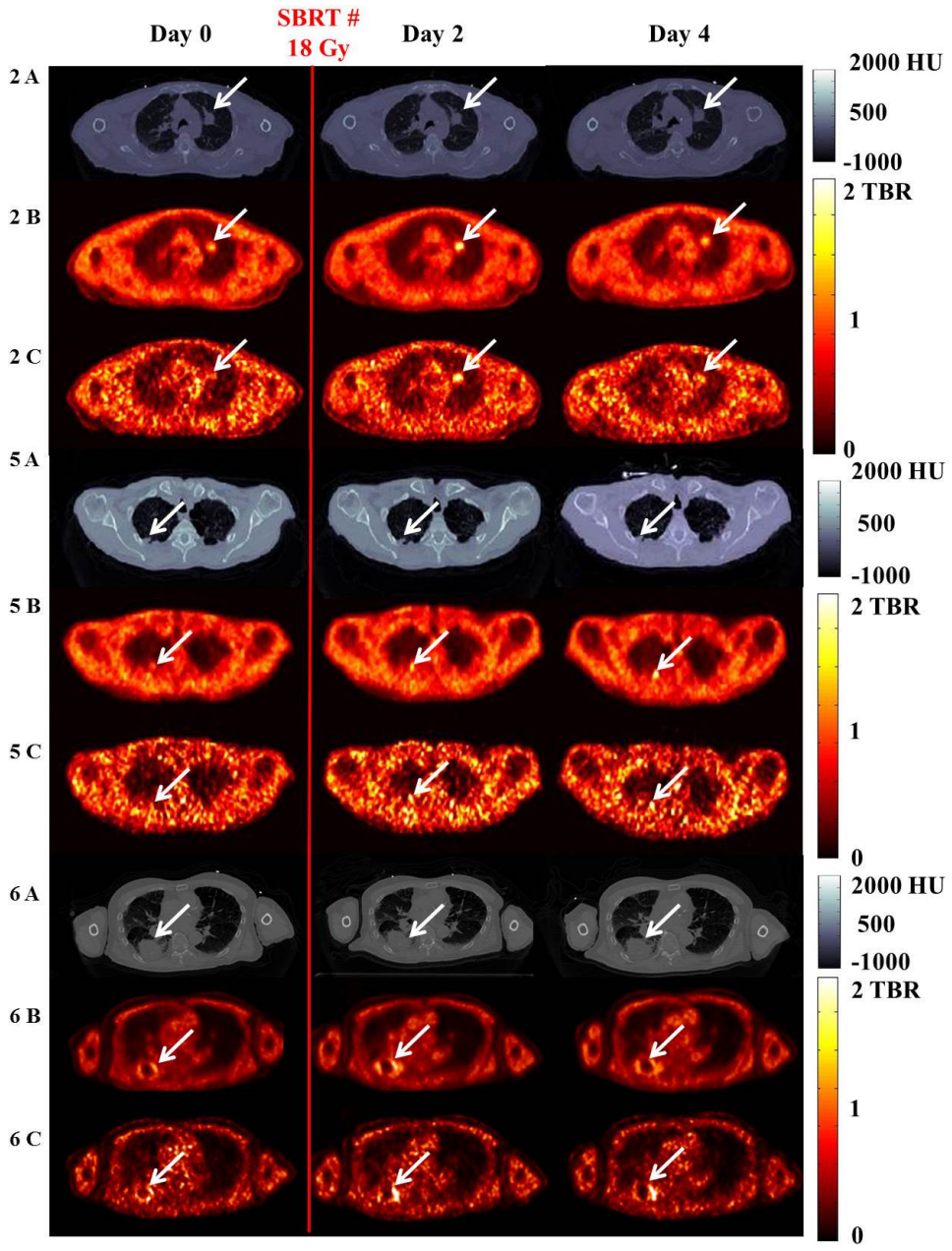

Figure 2.

Representative axial images for patients with baseline tumor hypoxia (patient 2 (2A-C), patient 5 (5A-C), and patient 6 (6A-C)) show variation in the tumor HV (day 0 to 4). Red vertical line indicates SBRT fraction delivery (18 or 10 Gy) immediately after day 0 imaging. Rows (A) show CT images (scale bar in Hounsfield Units [HU]). Rows (B) and (C) show ungated and respiratory-corrected PET images. Arrows indicate the tumor or hypoxia. Scale bar in TBR (no units).

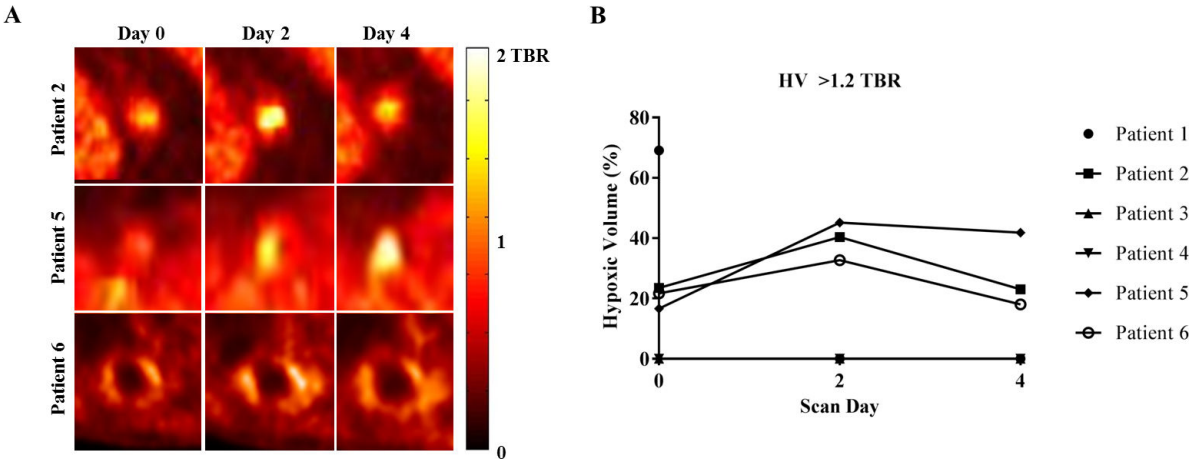

Figure 3.

(A) Enlarged axial PET images of patients with detectable baseline tumor hypoxia (patients 2, 5, and 6) **(B)** Temporal variation in tumor hypoxic volume defined by TBR >1.2 (all patients) calculated on respiratory-corrected images.

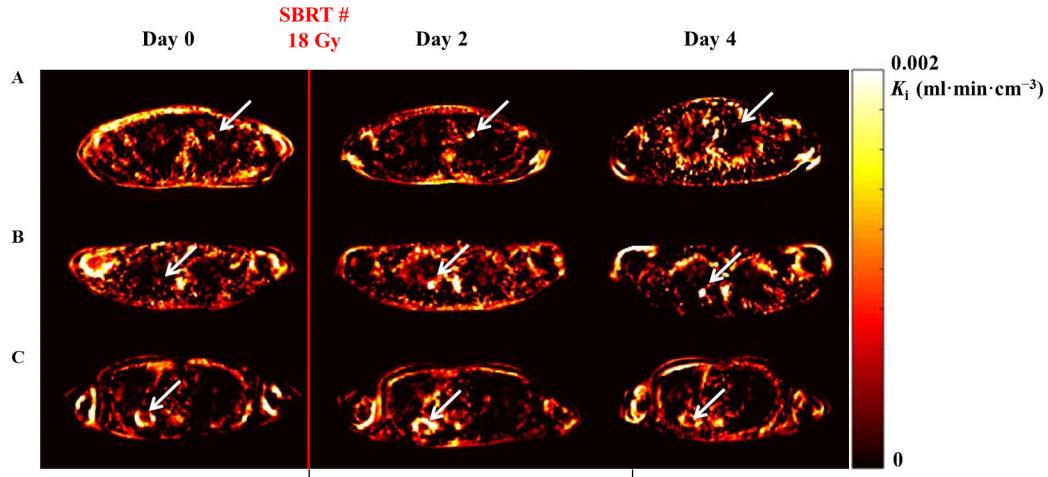

Patient	HV (%)*	Mean K_i	Max K_i	HV (%)*	Mean K_i	Max K_i	HV (%)*	Mean K_i	Max K_i
2	20.5	4.6×10^{-4}	2.5×10^{-3}	39.3	4.6×10^{-4}	4.3×10^{-3}	27.7	4.4×10^{-4}	3.9×10^{-3}
5	17.9	3.8×10^{-4}	3.1×10^{-3}	48.2	9.3×10^{-4}	4.7×10^{-3}	69.4	7.8×10^{-4}	8.8×10^{-3}
6	22.6	7.6×10^{-4}	4.2×10^{-3}	20.0	6.2×10^{-4}	4.4×10^{-3}	26.4	8.4×10^{-4}	4.1×10^{-3}

*Threshold = $K_i > 0.0015$ (ml·min·cm^{-3})

Figure 4.

Patlak ($t^* = 40$ min) tracer kinetic analysis of ^{18}F-FMISO. **Top panel:** Axial K_i parametric maps (calculated on ungated images) of the rate of tracer influx K_i (mL·min· cm^{-3}) for patients 2 (row A), 5 (row B), and 6 (row C) showing variation in the hypoxic volume across imaging days. Arrows indicate location of hypoxia. K_i indicates hypoxia as yellow/white. **Bottom Panel:** HV (%), calculated using $K_i > 0.0015$ mL·min·cm^{-3}, mean and maximum K_i.

Table 1

Characteristics of all early-stage NSCLC patients with single tumor lesions undergoing SBRT and serial ^{18}F-FMISO-PET imaging.

Patient	Age	Gender	Histologic diagnosis	Stage (TNM)	Tumor diameter (cm)	Absolute vol. (cm^3)	Tumor location	Max motion (mm)	Prescription dose	Completed all FMISO PET
1	78	M	adenocarcinoma	stage IIA, cT2bN0M0	4.1	23	right upper lobe	8.8	18 Gy × 3	No
2	68	M	squamous cell carcinoma	stage IA, cT1bN0M0	2.2	8	left upper lobe	4.8	18 Gy × 3	Yes
3	75	M	adenocarcinoma	stage IA, pT1aN0	1.6	3	left lower lobe	12.4	18 Gy × 3	Yes
4	65	F	non-biopsied (ground glass based on imaging appearance)	stage IA, pT1bN0	2.5	5	right upper lobe	4.4	18 Gy × 3	Yes
5	66	M	non-biopsied	stage IA, pT1aN0	1.3	2	right upper lobe	2.6	18 Gy × 3	Yes
6	69	M	squamous cell carcinoma	stage IIB, T3N0	5.3	94	right lower lobe	14.6	10 Gy × 5	Yes

Int J Radiat Oncol Biol Phys. Author manuscript; available in PMC 2019 September 01.

Table 2

Temporal variation in tumor hypoxic volume defined by TBR >1.2, mean TBR, and maximum TBR for all patients calculated on respiratory-corrected images.

	Day 0	Day 2	Day 4
Patient	**HV (%)**		
1	69.1	–	–
2	23.5	40.4	23.1
3	0.0	0.0	0.0
4	0.0	0.0	0.0
5	16.6	45.2	41.9
6	21.7	32.7	18.1
Patient	**Mean TBR**		
1	1.26	–	–
2	0.60	0.87	0.68
3	0.51	0.50	0.59
4	0.39	0.37	0.32
5	0.63	0.84	0.84
6	0.84	0.98	0.90
Patient	**Maximum TBR**		
1	4.25	–	–
2	3.12	3.00	2.30
3	0.93	0.90	1.02
4	1.02	1.11	1.00
5	2.74	3.31	3.99
6	2.66	3.08	2.90